Electronic Structure of Halogen-Substituted Methyl Radicals: Equilibrium Geometries and Vibrational Spectra of CH_2Cl and CH_2F

Sergey V. Levchenko and Anna I. Krylov*

Department of Chemistry, University of Southern California, Los Angeles, California 90089-0482

Received: January 29, 2002

Anharmonic corrections for the out-of-plane (OPLA) vibrational modes of CH_2Cl, CH_2F, and CH_3 radicals have been calculated. For these radicals, it is possible to describe the OPLA motion within a simple one-dimensional model based on the adiabatic separation of the (slowest) OPLA mode from all other vibrations. The effective potentials have been calculated by CCSD(T) and DFT/B3LYP methods with 6-311(+,+)G(3df,2pd) basis sets. It is found that halogen substitution increases the anharmonicities dramatically, i.e., from 19% in CH_3 up to about ±100% in CH_2Cl and CH_2F. The resulting frequencies of the fundamental OPLA transition are in good agreement with the experimental values. In the case of CH_2F, the large anharmonicity in the OPLA mode results in a wave function delocalized over the two minima of the double well potential. This reconciles the experimentally determined planar (C_{2v}) structure with the calculated pyramidal (C_s) equilibrium geometry.

I. Introduction

The methyl radical in its ground electronic state possesses a rather rigid, planar (D_{3h}) structure, and the frequency of its out-of-plane (OPLA) vibration is about 600 cm^{-1}.[1−5] This is easily rationalized in terms of hybridization theory: the unpaired electron occupies the $2p_z$ orbital of carbon, while the 2s, $2p_x$, and $2p_y$ orbitals form three equivalent σ_{CH} bonds (sp^2-hybridization). Obviously, the repulsion between the unpaired electron and those involved in the CH bonds is minimal for the planar structure, and it rapidly increases for large amplitude OPLA displacements. That is why the anharmonicity of the OPLA mode is *negative* (i.e., the potential steepness increases with a vibrational excitation), as opposed to the *positive* anharmonicity found for a stretching Morse-type potential. Such anharmonicity (about 11% from the experimental fundamental frequency ω_{01} value) for the OPLA mode of the methyl radical has been postulated by Riveros[6] in order to explain the deviation of the observed[2] isotope shifts of the OPLA fundamentals from the values calculated assuming a planar structure[1] and harmonic OPLA motion.

When one or more hydrogen atoms are substituted by halogens, the interaction of the lone pairs of the latter with the unpaired electron changes the bonding considerably: the carbon−halogen bonds contract and the corresponding force constants increase,[7−11] some radicals assume pyramidal structures,[7,8] etc. (see ref 12 for a summary of the spectroscopic data). Recently, in collaboration with Reisler and co-workers, we have analyzed[13,14] the bonding in the ground and electronically excited states of CH_2X (X = F, Cl) radicals: our ab initio calculations have shown[13] that a $^1/_2$(n−p)-π bond forms between the chlorine and carbon atoms in CH_2Cl, whereas in CH_2F no significant electron delocalization is obtained because of the much larger difference in the electronegativities of carbon and fluorine. The present work demonstrates that halogen substitution also increases dramatically the anharmonicity of the OPLA mode.

Electronic structure calculations of halogen-substituted methyl radicals are difficult.[15−19] The ground state equilibrium geometries and frequencies of well-behaved molecules are usually reproduced accurately by high-level ab initio calculations, e.g., coupled-cluster method with single and double substitutions (CCSD)[20] and perturbative account of triple excitations [CCSD(T)].[21] However, in the case of halogen-substituted methyl radicals, the discrepancy between theory and experiment is alarmingly large: while theory predicts nonplanar structures,[15,17−19] the experiments consistently yield planar geometries with well-defined minima.[22−27] For example, the calculated equilibrium geometry of the CH_2F radical deviates from the experimentally determined[22−24] planar structure by 30°,[17−19] and the calculated harmonic frequency of the umbrella mode is twice higher than the experimental value of the ω_{01} transition.[23,24] In the case of CH_2Cl, the situation is reversed: the calculated harmonic frequency is twice *lower* than the experimental ω_{01}.[9,10]

The main purpose of the present study is to identify the origin of this large discrepancy, e.g., a failure of ab initio theory, an erroneous interpretation of the experiment, or unexpected subtleties in the electronic structure of these seemingly simple species. Indeed, the results of ab initio calculations for open-shell species have to be scrutinized carefully; in addition to the obvious observation that the requirements for the one-particle basis set are higher than for closed shell molecules (due to the more diffuse nature of the unpaired electron), the doublet radicals are known to exhibit artifactual spatial symmetry breaking,[28] which often results in anomalous vibrational frequencies and incorrect structures.[29−40]

We have found that the potential energy surfaces of CH_2X and CH_3 radicals are described accurately by CCSD(T) theory, and that the source of the discrepancy mentioned above is in the anomalously large anharmonicity in the OPLA mode, which is roughly equal to the harmonic frequency. Density functional theory (DFT)[41] with B3LYP exchange-correlation functional[42] yields similar results. The good performance of DFT/B3LYP is in agreement with recent benchmark studies of the equilibrium properties of doublet radicals.[43−45]

There are numerous examples of highly anharmonic systems, especially among van der Waals clusters. In the extreme case

10.1021/jp020275w CCC: $22.00
Published on Web 04/18/2002

of weekly interacting He atoms, the zero-point energy is so high that the vibrational wave function is delocalized over several minima of the potential energy surface and, therefore, bears no resemblance to localized harmonic wave functions.[46] In the less dramatic case of Ar clusters, the anharmonic corrections change the values of the fundamental transitions by 10−25% of the corresponding harmonic frequencies.[47] Large anharmonicities, i.e., up to 100%, have been reported for the *inter*molecular modes in water clusters.[48] However, the anharmonicities of *intra*molecular vibrations are usually much smaller: 1−5% is a typical value.[45,49−55,56−58] In this context, the anharmonicities of the OPLA motion in the halogen-substituted methyl radicals are exceptionally large.

The paper is organized as follows: section II describes the theoretical model, section IIIA outlines the computational details, sections IIIB, IIIC, and IIID present the calculated equilibrium structures and vibrational spectra. Our final remarks and conclusions are given in section IV.

II. Theory

In very small systems, where it is possible to obtain a nearly global analytic fit of the multidimensional surface, the vibrational problem can be solved with very high accuracy.[52] In polyatomic systems, the moderate anharmonicity can be accounted for by calculating higher, i.e., third and fourth, derivatives with subsequent second-order perturbative theoretical treatment of the fundamental vibrational frequencies.[49−51,53,56−59] To treat systems with larger anharmonicities, the vibrational self-consistent field (VSCF) method can be applied.[60−63] The approximation recently proposed by Chaban and Gerber for multidimensional integral evaluation has enabled the application of the VSCF method to very large systems.[54,55] Below we outline a less general approach, which can be employed to calculate the vibrational wave functions for OPLA motions in CH_2X radicals. A similar strategy has been employed by Johnson and Hudgens in their calculations of anharmonic effects in the CH_2-OH radical.[64]

For an M-atomic system, it is customary to use normal coordinates $\{Q_i\}_{i=1}^{N}$ (where $N = 3M - 6$ for a nonlinear molecule). The nonunitary transformations between Cartesian ($\{X_i\}_{i=1}^{3M}$) and normal ($\{Q_i\}_{i=1}^{N}$) coordinates are defined as follows:

$$Q_i = \sum_{j=1}^{3M} R_{ij} X_j \tag{1}$$

$$X_i = \sum_{j=1}^{N} L_{ij} Q_j \tag{2}$$

$$\mathbf{RL} = \mathbf{I} \tag{3}$$

where $\mathbf{I}$ is an $N \times N$ unit matrix, $I_{ij} = \delta_{ij}$. The transformation matrixes $\mathbf{R}$ ($N \times 3M$) and $\mathbf{L}$ ($3M \times N$) are found by solving the normal mode problem:

$$\mathbf{UL} = \mathbf{TL}\Lambda \qquad \Lambda_{ij} = \delta_{ij}\omega_i^2 \tag{4}$$

$$\mathbf{L}^{+}\mathbf{TL} = \mathbf{I} \tag{5}$$

$$\mathbf{R} = \mathbf{L}^{+}\mathbf{T} \tag{6}$$

where $\mathbf{T}$ is a diagonal matrix composed of atomic masses, ω_i is the vibrational frequency of mode i, and $\mathbf{U}$ is the Hessian matrix evaluated at the equilibrium geometry $\{X_i^{eq}\}$:

$$U_{ij} = \frac{\partial^2 V(X_1^{\mathrm{eq}},...,X_{3M}^{\mathrm{eq}})}{\partial X_i \partial X_j} \tag{7}$$

In normal coordinates, the Schrödinger equation for the N-dimensional vibrational wave function $\Psi(Q_1,...,Q_N)$ reads

$$\left(-\frac{1}{2}\sum_{i=1}^{N}\frac{\partial^2}{\partial Q_i^2} + V(Q_1,...,Q_N)\right)\Psi_n(Q_1,...,Q_N) = E_n\Psi_n(Q_1,...,Q_N), \tag{8}$$

where $V(Q_1,...,Q_N)$ is the full potential energy surface, and atomic masses have been absorbed into the transformation $\mathbf{R}$ from eq 1. In the spirit of the VSCF approximation, we employ a separable ansatz for the wave function:

$$\Psi_n(Q_1,...,Q_N) = \xi_{n'}(\theta)\cdot\Phi_{n''}(Q_2,...,Q_N) \tag{9}$$

where $\theta \equiv Q_1$ is the normal coordinate of the OPLA mode. The wave functions $\xi_{n'}(\theta)$ and $\Phi_{n''}(Q_2,...,Q_N)$ are defined by the two coupled equations:

$$\left(-\frac{1}{2}\frac{\partial^2}{\partial\theta^2} + V_\Phi(\theta)\right)\xi_{n'}(\theta) = \epsilon_{n'}\xi_{n'}(\theta) \tag{10}$$

$$\left(-\frac{1}{2}\sum_{i=2}^{N}\frac{\partial^2}{\partial Q_i^2} + V_\xi(Q_2,...,Q_N)\right)\Phi_{n''}(Q_2,...,Q_N) = \epsilon_{n''}\Phi_{n''}(Q_2,...,Q_N) \tag{11}$$

where $V_\Phi(\theta)$ and $V_\xi(Q_2,...,Q_N)$ are the mean-field potentials:

$$V_\Phi(\theta) = \langle\Phi(Q_2,...,Q_N)|V(\theta,Q_2,...,Q_N)|\Phi(Q_2,...,Q_N)\rangle_{Q_2,...,Q_N} \tag{12}$$

$$V_\xi(Q_2,...,Q_N) = \langle\xi(\theta)|V(\theta,Q_2,...,Q_N)|\xi(\theta)\rangle_\theta \tag{13}$$

Since we are interested in the OPLA fundamental only (i.e., $n' = 0, 1$), all the other vibrational degrees of freedom can be assumed to be in their ground state. That is why only the lowest $\Phi_{n''}(Q_2,...,Q_N)$ is needed, i.e., $n'' = 0$.

At this point, we introduce additional approximations to the mean-field separation of the OPLA motion. Instead of solving eqs 10−13 self-consistently, we assume that the wave function $\Phi(Q_2,...,Q_N)$ has the following simple form:

$$\Phi(Q_2,...,Q_N) = \prod_{i=2}^{N}\delta(Q_i - Q_i^{\mathrm{opt}}), \tag{14}$$

where δ stands for the δ-function, and the choice of optimal coordinates $\{Q_i^{\mathrm{opt}}\}_{i=2}^{N}$ is described below. With this approximation, the effective potential for the OPLA motion assumes the following form:

$$V_\Phi(\theta) \approx V(\theta,Q_2^{\mathrm{opt}},...,Q_N^{\mathrm{opt}}) \tag{15}$$

We consider two different choices of parameters $\{Q_i^{\mathrm{opt}}\}_{i=2}^{N}$ from eqs 14 and 15. The first model completely neglects the interaction between modes, and thus assumes that when atoms move along the OPLA coordinate, all the other coordinates do not change, i.e., $Q_i^{\mathrm{opt}} \equiv Q_i^{\mathrm{eq}}$:

$$V_\Phi(\theta) \approx V(\theta,Q_2^{\mathrm{eq}},Q_3^{\mathrm{eq}},...,Q_N^{\mathrm{eq}}) \tag{16}$$

TABLE 1: Calculated Ground State Geometries of CH_2X (X = Cl, F, H) Radicals

	symm	r_{CH}, Å	r_{CX}, Å	α_{HCH}	Θ^b	E_{nuc}	E_{tot}
			CCSD(T)/6-311(+,+)G(3df,3pd)[a]				
CH_2Cl (X^2B_1)	C_{2v}	1.076	1.691	124.17	180	45.620 937	−499.007 703
CH_2F (X^2A')	C_s	1.079	1.335	124.11	153.11	32.246 535	−138.935 120
CH_2F (X^2B_1)	C_{2v}	1.076	1.332	127.60	180	32.274 065	−138.934 617
CH_3 (X^2A_2'')	D_{3h}	1.0783		120	180	9.683 711	−39.783 994
			DFT(B3LYP)/6-311(+,+)G(3df,3pd)[a]				
CH_2Cl (X^2B_1)	C_{2v}	1.076	1.698	124.41	180	45.479 968	−499.490 818
CH_2F (X^2A')	C_s	1.079	1.338	125.13	156.70	32.180 494	−139.128 583
CH_2F (X^2B_1)	C_{2v}	1.076	1.336	127.79	180	32.201 855	−139.128 331
CH_3 (X^2A_2'')	D_{3h}	1.0779		120	180	9.687 270	−39.858 366

[a] Pure angular momentum spherical harmonics are used. [b] Dihedral HCXH angle.

TABLE 2: Ground State Rotational Constants (MHz) for CH_2X Radicals (X = Cl, F, H)[a]

method	*A*	*B*	*C*
		CH_2Cl	
CCSD(T)/C_{2v}	277 359	16 016.398	15 142.006
DFT(B3LYP)/C_{2v}	277 071	15 899.166	15 036.336
exp[25]	274 380 ± 78	15 948.0282 ± 126	15 057.0443 ± 123
		CH_2F	
CCSD(T)/C_{2v}	268 993	31 177.081	27 938.892
CCSD(T)/C_s	264 292	31 102.495	28 074.005
DFT(B3LYP)/C_{2v}	268 352	31 019.521	27 805.420
DFT(B3LYP)/C_s	264 835	30 962.334	27 904.259
exp[23]	265 200	30 948.322(27)	27 727.773(27)
		CH_3	
CCSD(T)/D_{3h}	287 526.470	287 526.470	143 763.235
DFT(B3LYP)/D_{3h}	287 738.378	287 738.163	143 869.135
exp[5]	287 145(5)	287 145(5)	142 165(20)

[a] Theoretical values are calculated at the equilibrium geometries and therefore do not include vibrational averaging.

Drawing from the analogy with the electronic structure problem, we call eq 16 the *diabatic approximation*.

Alternatively, one can consider a model that assumes that the motions of all the other coordinates are much faster than that of the OPLA vibration. In this model, all the other degrees of freedom can simultaneously adjust to the current value of the OPLA coordinate. Thus, $\{Q_i^{opt}\}_{i=2}^N$ are found by optimizing the potential $V(\theta,Q_2,...,Q_N)$ with respect to $\{Q_i\}_{i=2}^N$ and at a fixed value of θ:

$$\frac{\partial V(\theta,Q_2,...,Q_N)}{\partial Q_i}\Big|_{Q_i=Q_i^{opt}} = 0, \qquad i = 2, ..., N \qquad (17)$$

We call this model the *adiabatic approximation*. The low frequency of the OPLA motion, which is at least twice slower than any other vibration in these radicals, justifies the adiabatic separation of the slow and fast motions. Due to symmetry considerations, the diabatic and adiabatic OPLA effective potentials have an identical harmonic part (see Appendix).

Our results show that the approximate account of the interaction between the modes in the adiabatic model yields a better agreement with the experiment. However, even the oversimplified diabatic model is capable of describing the anharmonicity in a qualitatively correct way.

III. Results and Discussion

A. Computational Details. We report results obtained with the CCSD(T)[21] and DFT/B3LYP[41,42] methods. The CCSD(T) calculations have been performed with the ACES II electronic structure program.[65] For DFT calculations, the Q-Chem ab initio package[66] has been used. All calculations employ the 6-311(+,+)G(3df,3pd) basis set, derived from the polarized split-valence 6-311G(d,p) basis[67,68] by augmenting it by additional sets of polarization and diffuse functions.[69,70] We find that the heavy polarization is crucial for the correct description of the equilibrium structures of halogen substituted methyl radicals: for example, CH_2Cl becomes pyramidal in smaller basis sets.

The CCSD(T) harmonic frequencies are calculated by using second analytic derivatives,[65] at the geometries optimized with the CCSD(T) method. Finite differences of analytically computed first-order derivatives are used to calculate the harmonic frequencies with the DFT/B3LYP method,[66] at the geometries optimized with DFT/B3LYP.

The optimized geometries of the CH_2X radicals are given in Table 1. The rotational constants calculated at these equilibrium geometries are summarized in Table 2. Since the calculated rotational constants are not vibrationally averaged, the comparison with experiment is not straightforward.

The procedure for calculating the one-dimensional diabatic and adiabatic effective potentials (eqs 15−17) is outlined below. First, geometry optimization with a C_{2v} symmetry constraint and normal-mode analysis are performed at each level of theory. This yields the transformation matrixes *R* and *L* from the eqs 1 and 2. Second, the equilibrium values of the normal coordinates, $\{Q^{eq}\}$, are calculated from the equilibrium values of the Cartesian coordinates, $\{X^{eq}\}$, by using eq 1. Finally, a grid of θ-values and the corresponding optimal values of the other coordinates, $\{Q_i^{opt}\}_{i=2}^N$, are generated and the total energies are computed at these points.

For the diabatic effective potentials, a nonuniform grid of displacements along θ (i.e., the OPLA normal coordinate) is generated. All the other normal coordinates are frozen at their equilibrium values. The corresponding Cartesian geometries are computed by using eq 2. To calculate the adiabatic effective potentials, a grid of values for the torsion angle is generated and the geometry is optimized with respect to all the other

TABLE 3: $CH_2Cl^•$ Calculated Harmonic Vibrational Frequencies ω_e and Experimental Values ω_{01}, cm^{-1} [a]

method	CCl stretch a_1	CH_2 scissors a_1	OPLA b_1	CH_2 rock b_2	CH_2 s-stretch a_1	CH_2 a-stretch b_2
CCSD(T)	868 (5%)	1434 (3%)	168 (58%)	1004	3179	3335
DFT	835 (1%)	1415 (2%)	229 (43%)	997	3169	3320
exp	827[10,9]	1391[10]	402[10,9]			

[a] The relative differences, $\Delta = (\omega_e - \omega_{01})/\omega_{01}$•100%, are shown in parentheses.

TABLE 4: $CH_2Cl^•$ Parameters (10^{-6} a.u.) of the Analytical Fit (18) of the OPLA Effective Potentials

method	a_2	a_4	a_6	a_8
		Diabatic Potential		
CCSD(T)	0.295 18	0.003 054 44	-4.13673×10^{-7}	3.3010×10^{-11}
DFT	0.558 95	0.002 923 34	-3.86651×10^{-7}	2.8935×10^{-11}
		Adiabatic Potential		
CCSD(T)	0.294 43	0.001 181 34	-3.6527×10^{-8}	5.750×10^{-12}
DFT	0.544 87	0.001 092 29	-3.2434×10^{-8}	3.480×10^{-12}

internal coordinates at each value of the torsion angle. By using the transformation matrix R from eq 1, these Cartesian coordinates are transformed to the normal coordinates. This yields values of the normal coordinate θ that correspond to a fixed torsion angle, and optimum values of all the other internal coordinates. This procedure is equivalent to a constrained geometry optimization in the normal coordinates, with the OPLA normal coordinate being frozen at a certain value of θ.

The energy points calculated in this way are then used to determine the parameters of the following analytical form of the effective potential:

$$V(\theta) = a_2\theta^2 + a_4\theta^4 + a_6\theta^6 + a_8\theta^8 \qquad (18)$$

The analytical fit of the potential allows extrapolation of the potential function beyond the range in which the energy points are calculated. We have found that powers of θ higher than fourth are necessary for an accurate fit, e.g., to reproduce the correct second derivative of the effective potentials. The harmonic frequencies of our effective OPLA potentials parametrized by eq 18 agree within 1 cm^{-1} with the harmonic frequencies calculated by solving the normal mode problem at the optimized geometry.

Anharmonic frequencies, ω_{01}, are calculated by numerically solving the one-dimensional Schrödinger eq 10 with potentials (18) by using the program LEVEL.[71]

B. CH_2Cl. The calculated harmonic frequencies of the CH_2-Cl radical are summarized in Table 3. The deviation of the calculated harmonic frequencies from the corresponding experimental values does not exceed 5% for the CCl stretch and CH_2 scissors. However the calculated value of the OPLA harmonic frequency is twice lower than the experimental value of ω_{01}. The agreement between the calculated and the experimental values seems to be better for DFT/B3LYP than for the reliable and accurate CCSD(T) method.

The parameters of the analytical fit of the diabatic and adiabatic effective potentials (see section II) are given in Table 4. The CCSD(T) adiabatic effective potential is shown in Figure 1, along with the corresponding harmonic potential (dashed line). Figure 1 illustrates the strikingly large negative anharmonicity of the OPLA vibrational mode of CH_2Cl. The calculated value of the 0−1 OPLA transition is 422 cm^{-1}, more than twice higher than the harmonic frequency of 168 cm^{-1}. The former is in a good agreement with the experimental value of 402 cm^{-1}. The DFT/B3LYP adiabatic effective potential yields a similar value (434 cm^{-1}). Therefore, both models give anharmonic corrections to the OPLA mode of CH_2Cl that are roughly equal in magnitude

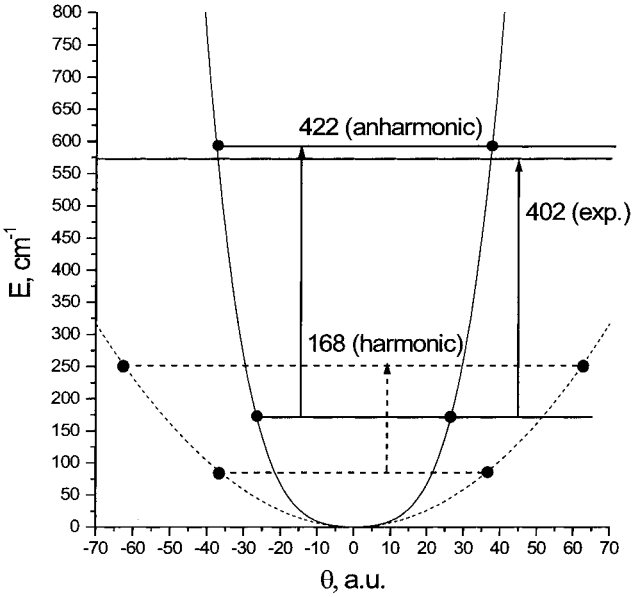

Figure 1. Harmonic (dashed line) and anharmonic (solid line) OPLA adiabatic effective potentials for the CH_2Cl radical [CCSD(T)/6-311(+,+)G(3df,3pd)]. The positions of the zero and first excited vibrational levels are shown by horizontal lines. The calculated and experimental values for the fundamental transition are shown by vertical arrows.

to the harmonic frequency. The OPLA fundamental transition energy calculated by CCSD(T) deviates from the experiment by 5%, and the DFT/B3LYP value by 8%. The amplitude of the zero point motion for the OPLA mode is rather large: the turning points of the anharmonic potential from Figure 1 correspond to a 26° deviation from a planar structure.

As expected, the diabatic effective potentials are too steep because the relaxation in the other coordinates is neglected. Thus, the diabatic model overestimates the anharmonicities. The values of the diabatic ω_{01} are 543 and 554 cm^{-1} for the CCSD(T) and DFT/B3LYP methods, respectively. Nevertheless, even this oversimplified model produces a better estimate for ω_{01} than the harmonic model.

It is interesting to compare our OPLA effective potential with that reconstructed by Andrews and Smith.[10] Their anharmonic quartic potential has been parametrized to reproduce the OPLA vibrational frequencies of the deuterated CH_2Cl radicals. The harmonic frequency calculated with their potential is 262 cm^{-1}. This value is 94 cm^{-1} above the CCSD(T) harmonic frequency of 168 cm^{-1}. This large discrepancy is due to the absence of higher powers of θ in their effective potential.

C. CH_2F. The calculated harmonic frequencies for the CH_2F radical are presented in Table 5. For this radical, the OPLA harmonic frequency calculated at the optimized equilibrium geometry (C_s structure) is about twice higher than the experimental ω_{01} for the OPLA fundamental transition (Hudgens et al. recommend 260 ± 30 cm^{-1},[24] and Endo et. al. recommend 300 ± 30 cm^{-1} [23]). This situation is exactly the reverse of that in the CH_2Cl radical, where the harmonic OPLA frequency is twice lower than the experimental ω_{01}. Similarly to CH_2Cl, the

TABLE 5: $CH_2F^\bullet$ Calculated Harmonic Vibrational Frequencies ω_e and Experimental Values ω_{01}, cm^{-1} [a]

method	CF stretch a_1	CH_2 scissors a_1	OPLA b_1	CH_2 rock b_2	CH_2 s-stretch a_1	CH_2 a-stretch b_2
CCSD(T)/C_{2v}	1208 (3%)	1478 (2%)	437i	1167	3173	3347
DFT/C_{2v}	1184 (1%)	1439 (5%)	361i	1130	3120	3290
CCSD(T)/C_s	1199 (2%)	1482 (2%)	585 (95%)	1185	3142	3302
DFT/C_s	1177 (0.6%)	1440 (5%)	482 (61%)	1142	3093	3254
exp	1170[91,92]	1515[92]	300 ± 30[23,24]			

[a] The relative differences, $\Delta = (\omega_e - \omega_{01})/\omega_{01}\cdot 100\%$, are shown in parentheses.

TABLE 6: $CH_2F^\bullet$ Parameters (10^{-6} a.u.) of the Analytical Fit (18) of the OPLA Effective Potentials

method	a_2	a_4	a_6	a_8
		Diabatic Potential		
CCSD(T)	−1.988 28	0.003 721 25	$-5.589\,76 \times 10^{-7}$	$5.335\,84 \times 10^{-11}$
DFT	−1.318 26	0.003 365 44	$-4.555\,63 \times 10^{-7}$	$3.458\,19 \times 10^{-11}$
		Adiabatic Potential		
CCSD(T)	−1.986 33	0.002 059 17	$-2.055\,65 \times 10^{-7}$	2.8313×10^{-11}
DFT	−1.312 81	0.001 754 63	$-1.225\,98 \times 10^{-7}$	1.1967×10^{-11}

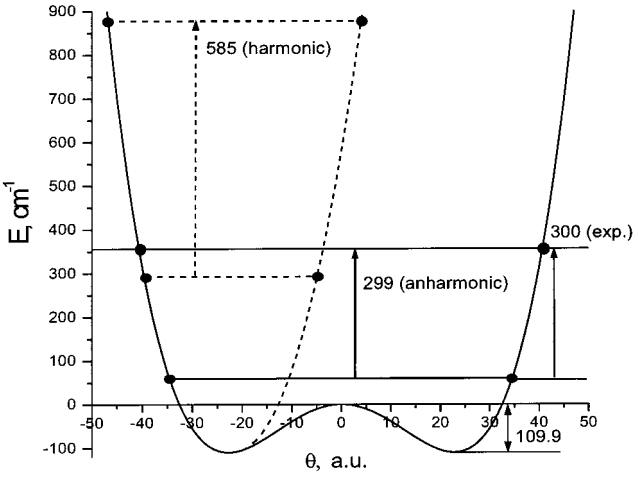

Figure 2. Anharmonic (solid line) OPLA adiabatic effective potential for the CH_2F radical [CCSD(T)/6-311(+,+)G(3df,3pd)]. The dashed curve represents the harmonic part of the potential at the optimized nonplanar (C_s) geometry. The corresponding harmonic frequency is also shown. The negative curvature at the planar (C_{2v}) geometry (i.e., at the barrier) yields the imaginary frequency of 437i cm^{-1}. The positions of the zero and first excited levels are shown by horizontal lines. The calculated and experimental values of the OPLA fundamental transition are shown by vertical arrows.

discrepancy between the theoretical harmonic frequencies and the experimental value of ω_{01} is larger for CCSD(T) than for DFT.

The parameters of the analytical fit of the diabatic and adiabatic effective potentials (see section II) are given in Table 6. The CCSD(T) adiabatic effective potential is shown in Figure 2, as well as the corresponding harmonic potential. As shown in Figure 2, the zero-point vibrational level is 57 cm^{-1} above the barrier between the two nonplanar (C_s) minima. The amplitude of the zero-point OPLA vibration of CH_2F is very large: the turning points of the effective potential (Figure 2) correspond to the 38° deviation from the planar structure (vs 26° in CH_2Cl).

These results reconcile the theoretical predictions of a nonplanar equilibrium structure (with a deviation from planarity of about 27°) with the experimental results (microwave spectroscopy) that strongly support a C_{2v} symmetry.[22,23] Planar or near-planar (<5° deviation from planarity) geometry has also been suggested by the electron spin-resonance (ESR) study of Fessenden and Schuler.[72] A double-well potential with two strongly nonplanar minima has been ruled out as inconsistent with the measured value of the carbon hyperfine coupling constant:[72] even with the zero-point energy being above the barrier, the large-amplitude zero-point vibrations in the double well potential were estimated to cause a large increase in the vibrationally averaged carbon hyperfine coupling constant (thus revealing the nonplanar equilibrium structure of the radical). However, that estimate was based on the complete orbital following model,[73] which was shown to fail in similar circumstances, i.e., for the CH_3 radical.[74] To check the validity of the complete orbital following assumption, we performed Natural Bond Orbital analysis[75] of the CH_2F density at the optimized (strongly nonplanar) geometry. We find that the unpaired electron has only 6% s-character, whereas the complete orbital following model predicts about 14% s-character.[73,76] This demonstrates incomplete orbital following and reconciles the small value of the carbon hyperfine coupling constant[72] with the large amplitude zero-point OPLA motion in the double-well potential shown in Figure 2.

The calculated value of ω_{01}, 299 cm^{-1} [CCSD(T), adiabatic model] is in the excellent agreement with the experimental value of about 300 cm^{-1} [23,24](Figure 2). The adiabatic DFT potential results in a slightly higher value of 332 cm^{-1}. Similarly to the CH_2Cl case, the diabatic model overestimates the frequencies. A better performance of the adiabatic separation of the OPLA motion in CH_2F has been anticipated, because of the larger difference in frequencies between the OPLA vibration and all the other modes.

For CH_2F, the difference between the harmonic and anharmonic wave functions is even more dramatic than for CH_2Cl. The harmonic frequency is either too high (if calculated at the optimized C_s geometry), or imaginary (if calculated at the optimized C_{2v} geometry). These frequencies reflect the large local curvature at the C_s stationary point or the negative curvature at the barrier, but have no relation to the real vibrational levels of CH_2F.

D. CH_3. Table 7 summarizes the calculated CH_3 harmonic frequencies and the experimental values of its fundamental transitions. For CH_3, the discrepancy between the calculated harmonic OPLA frequencies and the experimental value of the transition energy ω_{01} is not as remarkable as it is for CH_2Cl and CH_2F. Nevertheless, the relative difference is still at least four times larger than for any other mode. As seen from the Table 7, this discrepancy is larger for CCSD(T) than for DFT (16% versus 11%). Since the molecule has been extensively studied both theoretically[77−79] and experimentally,[4−6,80−90] it is instructive to investigate how our model performs in this case.

The CCSD(T)/6-311(+,+)G(3df,3pd) harmonic OPLA frequency is 507 cm^{-1}, which is considerably lower than the harmonic frequency of 544 cm^{-1} derived from the Riveros fit.[6] Moreover, improving the one-electron basis set further lowers the harmonic frequency, e.g., the CCSD(T)/aug-cc-pVTZ value is 497 cm^{-1}.[79] Similarly to the CH_2Cl case, we attribute this difference to the absence of higher than quartic terms in the Riveros potential.

TABLE 7: $CH_3^•$ Calculated Harmonic Vibrational Frequencies ω_e and Experimental Values ω_{01}, cm^{-1} [a]

method	CH stretch a_1'	CH_2 scissors & rock e'	OPLA a_2''	CH_2 s,a-stretch e'
CCSD(T)	3104 (3%)	1424 (2%)	507 (16%)	3293 (4%)
DFT	3109 (3%)	1408 (0.4%)	542 (11%)	3287 (4%)
exp	3004[80−83]	1402[84,85]	607[5,4]	3161[86−90,85]

[a] The relative differences, $\Delta = (\omega_e - \omega_{01})/\omega_{01}$•100%, are shown in parentheses.

TABLE 8: $CH_3^•$ Parameters (10^{-6} a.u.) of the Analytical Fit (18) of the OPLA Effective Potentials

method	a_2	a_4	a_6	a_8
		Diabatic Potential		
CCSD(T)	2.670 68	0.002 523 17	-3.0602×10^{-7}	2.468×10^{-11}
DFT	3.069 87	0.002 300 44	-2.1121×10^{-7}	3.74×10^{-12}
		Adiabatic Potential		
CCSD(T)	2.668 94	0.001 512 57	-1.3727×10^{-7}	2.243×10^{-11}
DFT	3.107 64	0.001 248 58	-4.33×10^{-9}	8.17×10^{-12}

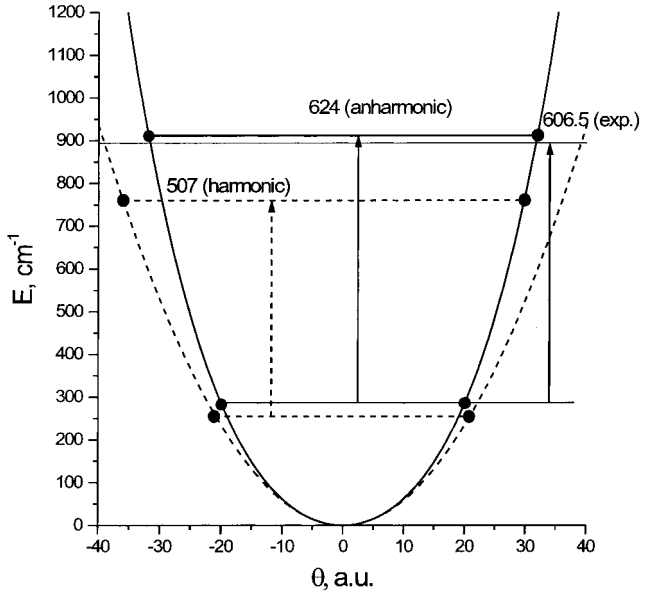

Figure 3. Harmonic (dashed line) and anharmonic (solid line) OPLA adiabatic effective potentials for the CH_3 radical [CCSD(T)/6-311(+,+)G(3df,3pd)]. The positions of the zero and first excited levels are shown by horizontal lines. The calculated and experimental values for the OPLA fundamental transition are shown by vertical arrows.

The parameters for the analytical fit of the diabatic and adiabatic effective potentials (see section II) are given in Table 8. The CCSD(T) adiabatic effective potential is shown in Figure 3, as well as the corresponding harmonic potential. The corresponding anharmonic frequency is 624 cm^{-1}. The adiabatic DFT value is 645 cm^{-1}. The deviation of the adiabatic anharmonic ω_{01} from the experiment is thus 4.5% for CCSD(T), and 6% for DFT model. As in the previous two cases, the anharmonic frequencies calculated using the diabatic effective potential overestimate the experimental transition energy by about 11% for CCSD(T), and 14% for DFT method.

Even though the frequency of the OPLA motion is higher than in CH_2Cl, the amplitude of the zero-point motion in the potential shown in Figure 3 is almost the same as in the case of CH_2Cl: the turning points correspond to a 25° deviation from planarity (vs 26° in CH_2Cl).

IV. Conclusions

We find large anharmonic corrections for the OPLA vibrational mode of the CH_2Cl, CH_2F, and CH_3 radicals. For these radicals, it is possible to describe the OPLA motion within a simple one-dimensional model on the basis of the adiabatic separation of the (slowest) OPLA mode from all the other vibrations. The OPLA vibrational frequencies of all three radicals are summarized in Tables 9 and 10. We find that halogen substitution increases the anharmonicities dramatically, i.e., from 19% in CH_3 up to about ±100% in CH_2Cl and CH_2F. The resulting frequencies of the fundamental OPLA transitions are in good agreement with the experimental values (the deviations are about 5%, similar to the other modes). In the case of CH_2F, the large anharmonicity in the OPLA mode results in a wave function delocalized over two minima of the double well potential. This reconciles the experimentally determined planar (C_{2v}) structure with the calculated pyramidal (C_s) equilibrium geometry.

TABLE 9: Calculated and Experimental Values for the OPLA Fundamental Transition, cm^{-1} [a]

species	ω_e	ω_{01}^{diab}	ω_{01}^{adiab}	exp
CH_2Cl	168	543	422	402
CH_2F	437i	419	299	300 ± 30
CH_3	507	672	624	607

[a] The OPLA adiabatic and diabatic effective potentials are calculated at the CCSD(T)/6-311++G(3df,3pd) level of theory.

TABLE 10: Calculated and Experimental Values for the OPLA Fundamental Transition, cm^{-1} [a]

species	ω_e	ω_{01}^{diab}	ω_{01}^{adiab}	exp
CH_2Cl	229	554	434	402
CH_2F	361i	447	332	300 ± 30
CH_3	542	689	645	606

[a] The OPLA adiabatic and diabatic effective potentials are calculated at the DFT(B3LYP)/6-311++G(3df,3pd) level of theory.

As demonstrated in Tables 9 and 10, the agreement of the CCSD(T) model with the experiment is consistently better than that of DFT. Nevertheless, DFT/B3LYP also yields reasonably accurate anharmonic potentials for the OPLA motion. This is consistent with other recent benchmark studies of radicals.[43,44]

Acknowledgment. We acknowledge support from the National Science Foundation CAREER Award (CHE-0094116), the Camille and Henry Dreyfus New Faculty Awards Program, and the donors of the Petroleum Research Fund, administered by the American Chemical Society. We wish to thank Prof. J. F. Stanton for giving us access to the ACES II ab initio program,[65] and for valuable help in setting up the calculations and resolving some problems. We are also grateful to Prof. H. Reisler and her group for stimulating discussions.

Appendix

Below we prove that the adiabatic and diabatic effective OPLA potentials (15) have identical harmonic parts. As a result, the approximate account of the interaction between modes by the adiabatic model affects only quartic and higher terms of the effective OPLA potential, leaving the harmonic part unchanged.

The proof is based on the following: (i) the OPLA normal mode does not belong to the fully symmetric irreducible representation (irrep) (e.g., it is b_1 in C_{2v} or a_2'' in D_{3h}), and (ii) the OPLA vibration is the only mode in this irrep. The above result is valid for any mode that satisfies (i) and (ii). However, for the sake of clarity the discussion below is focused on the specific case of the OPLA mode.

With (i) and (ii) satisfied for the OPLA mode, the global potential energy surface is symmetric with respect to positive and negative displacements along the OPLA coordinate:

$$V(\theta,Q_2,...,Q_N) = V(-\theta,Q_2,...,Q_N) \tag{19}$$

where θ denotes the normal coordinate for the OPLA motion. The potential along any fully symmetric coordinate is necessarily asymmetric (consider for example the symmetric CH stretch). Moreover, eq 19 would not hold if θ were not the only mode in its irrep, because the displacements along other modes from the same irrep would lower the symmetry of the system such that θ would become a fully symmetric coordinate at this reduced symmetry.

The derivative of the symmetric potential (19) with respect to any Q_i is also symmetric with respect to positive and negative distortions along θ:

$$\frac{\partial V(\theta,Q_2,...,Q_N)}{\partial Q_i} = \frac{\partial V(-\theta,Q_2,...,Q_N)}{Q_i} \tag{20}$$

Therefore, the $\{Q_i^{opt}\}_{i=2}^N$ defined by eq 17 are also even functions of θ:

$$Q_i^{opt}(\theta) = Q_i^{opt}(-\theta) \tag{21}$$

which means that the derivative of the $\{Q_i^{opt}(\theta)\}$ with respect to θ is zero at $\theta = 0$:

$$\frac{\partial Q_i^{opt}(\theta)}{\partial \theta}|_{\theta=0} = 0 \tag{22}$$

Let us now consider the Taylor expansion of the effective potential of eq 15, $V_\Phi(\theta)$, around $\theta = 0$ and analyze its quadratic terms with respect to θ. For the diabatic effective potential, we have

$$V_\Phi(\theta) \approx V(\theta,Q_2^{eq},...,Q_N^{eq})|_{\theta=0} + \frac{1}{2}\frac{\partial^2 V(\theta,Q_2^{eq},...,Q_N^{eq})}{\partial \theta^2}|_{\theta=0}\cdot\theta^2 + ... \tag{23}$$

where terms with higher powers of θ are neglected (the term linear in θ is absent because $\theta = 0$ corresponds to the equilibrium geometry, i.e., $\partial V/\partial\theta|_{\theta=0} = 0$). The potential above is simply the harmonic potential for the OPLA normal mode with the curvature defined by the second derivative at the equilibrium geometry.

Likewise, for the adiabatic effective potential we have

$$\begin{aligned} V(\theta,Q_2^{eq}(\theta),...,Q_N^{eq}(\theta)) \approx{}& V(\theta,Q_2^{eq},...,Q_N^{eq})|_{\theta=0} + \\ &\left(\frac{1}{2}\frac{\partial^2 V(\theta,Q_2^{eq},...,Q_N^{eq})}{\partial \theta^2}\Big|_{\theta=0} + \right. \\ &\sum_{i=2}^{N}\frac{\partial^2 V(\theta,Q_2^{eq},...,Q_N^{eq})}{\partial\theta\partial Q_i}\frac{\partial Q_i^{eq}(\theta)}{\partial\theta}\Big|_{\theta=0} + \\ &\frac{1}{2}\sum_{i,j=2}^{N}\frac{\partial^2 V(\theta,Q_2^{eq},...,Q_N^{eq})}{\partial Q_i\partial Q_j}\frac{\partial Q_i^{eq}(\theta)}{\partial\theta}\frac{\partial Q_j^{eq}(\theta)}{\partial\theta}\Big|_{\theta=0} + \\ &\left.\sum_{i=2}^{N}\frac{\partial V(\theta,Q_2^{eq},...,Q_N^{eq})}{\partial Q_i}\frac{\partial^2 Q_i^{eq}(\theta)}{\partial\theta^2}\Big|_{\theta=0}\right)\cdot\theta^2 + ... \end{aligned} \tag{24}$$

Taking into account eqs 22 and 17, one sees that the harmonic coefficients in eq 23 and eq 24 are identical.

References and Notes

(1) Fessenden, R. W. *J. Phys. Chem.* **1967**, *71*, 74.
(2) Milligan, D. E.; Jacox, M. E. *J. Chem. Phys.* **1967**, *47*, 5146.
(3) Herzberg, G. *Molecular spectroscopy and molecular structure; Electronic spectra end electronic structure of polyatomic molecules*; van Nostrand Reinhold: New York, 1966; Vol. III.
(4) Tan, L. Y.; Winer, A. M.; Pimentel, G. C. *J. Chem. Phys.* **1972**, *57*, 4028.
(5) Yamada, C.; Hirota, E.; Kawaguchi, K. *J. Chem. Phys.* **1981**, *75*, 5256.
(6) Riveros, J. M. *J. Chem. Phys.* **1969**, *51*, 1269.
(7) Carver, T. G.; Andrews, L. *J. Chem. Phys.* **1969**, *50*, 4235.
(8) Carver, T. G.; Andrews, L. *J. Chem. Phys.* **1969**, *50*, 4223.
(9) Jacox, M. E.; Milligan, D. E. *J. Chem. Phys.* **1970**, *53*, 2688.
(10) Andrews, L.; Smith, D. W. *J. Chem. Phys.* **1970**, *53*, 2956.
(11) Smith, D. W.; Andrews, L. *J. Chem. Phys.* **1970**, *58*, 5222.
(12) Jacox, M. E. *J. Phys. Chem. Ref. Data* **1994**, Monograph No. 3, p 1.
(13) Levchenko, S. V.; Krylov, A. I. *J. Chem. Phys.* **2001**, *115*, 7485.
(14) Dribinski, V.; Demyanenko, A.; Potter, A.; Reisler, H. *J. Chem. Phys.* **2001**, *115*, 7474.
(15) Li, Z.; Francisco, J. S. *J. Chem. Phys.* **1999**, *110*, 817.
(16) Morokuma, K; Pedersen, L.; Karplus, M. *J. Chem. Phys.* **1968**, *48*, 4801.
(17) Beveridge, D. L.; Dobosh, P. A.; Pople, J. A. *J. Chem. Phys.* **1968**, *48*, 4802.
(18) Konishi, H.; Morokuma, K. *J. Am. Chem. Soc.* **1972**, *94*, 5603.
(19) Bernardi, F.; Epiotis, N. D.; Cherry, W.; Schlegel, H. B.; Whangbo, M.-H.; Wolfe, S. *J. Am. Chem. Soc.* **1976**, *98*, 469.
(20) Purvis, G. D.; Bartlett, R. J. *J. Chem. Phys.* **1982**, *76*, 1910.
(21) Raghavachari, K.; Trucks, G. W.; Pople, J. A.; Head-Gordon, M. *Chem. Phys. Lett.* **1989**, *157*, 479.
(22) Mucha, J. A.; Jennings, D. A.; Evenson, K. M.; Hougen, J. T. *J. Mol. Spectrosc.* **1977**, *68*, 122.
(23) Endo, Y.; Yamada, C.; Saito, S.; Hirota, E. *J. Chem. Phys.* **1983**, *79*, 1605.
(24) Hudgens, J. W.; Dulcey, C. S.; Long, G. R.; Bogan, D. J. *J. Chem. Phys.* **1987**, *87*, 4546.
(25) Endo, Y.; Saito, S.; Hirota, E. *Can. J. Phys.* **1984**, *62*, 1347.
(26) Sears, T. J.; Temps, F.; Wagner, H. Gg.; Wolf, M. *J. Mol. Spectrosc.* **1994**, *168*, 136.
(27) Smith, D. W.; Andrews, L. *J. Chem. Phys.* **1971**, *55*, 5295.
(28) Davidson, E. R.; Borden, W. T. *J. Phys. Chem.* **1983**, *87*, 4783.
(29) Jackels, C. F.; Davidson, E. R. *J. Chem. Phys.* **1976**, *64*, 2908.
(30) Engelbrecht, L.; Liu, B. *J. Chem. Phys.* **1983**, *78*, 3097.
(31) McLean, A. D.; Lengsfield, B. H.; Pacansky, J.; Ellinger, Y. *J. Chem. Phys.* **1985**, *83*, 3567.
(32) Allen, W. D.; Horner, D. A.; DeKock, R. L.; Remington, R. B.; Schaefer, H. F., III. *Chem. Phys. Lett.* **1989**, *133*, 11.
(33) Kaldor, U. *Chem. Phys. Lett.* **1991**, *185*, 131.
(34) Stanton, J. F.; Gauss, J.; Bartlett, R. J. *J. Chem. Phys.* **1992**, *97*, 5554.
(35) Barnes, L. A.; Lindh, R. *Chem. Phys. Lett.* **1994**, *223*, 207.
(36) Xie, Y.; Allen, W. D.; Yamaguchi, Y.; Schaefer, H. F., III. *J. Chem. Phys.* **1996**, *104*, 7615.
(37) Hrušák, J.; Iwata, S. *J. Chem. Phys.* **1997**, *106*, 4877.
(38) Crawford, T. D.; Stanton, J. F.; Szalay, P. G.; Schaefer, H. F., III. *J. Chem. Phys.* **1997**, *107*, 2525.

(39) Crawford, T. D.; Stanton, J. F.; Allen, W. D.; Schaefer, H. F., III. *J. Chem. Phys.* **1997**, *107*, 10626.
(40) Crawford, T. D.; Stanton, J. F. *J. Chem. Phys.* **2000**, *112*, 7873.
(41) Parr, R. G.; Yang, W. *Density functional theory of atoms and molecules*, Vol. 16 of International Series of Monographs on Chemistry; Oxford: New York, 1989.
(42) Stephens, P. J.; Devlin, F. J.; Chabalowski, C. F.; Frisch, M. J. *J. Phys. Chem.* **1994**, *98*, 11623.
(43) Byrd, E. F. C.; Sherrill, C. D.; Head-Gordon, M. *J. Phys. Chem. A* **2001**, *105*, 9736.
(44) Cohen, R. D.; Sherrill, C. D. *J. Chem. Phys.* **2001**, *114*, 8257.
(45) Sinnokrot, M. O.; Sherrill, C. D. *J. Chem. Phys.* **2001**, *115*, 2439.
(46) Horn, T. R.; Gerber, R. B.; Ratner, M. A. *J. Chem. Phys.* **1989**, *91*, 1813.
(47) Jung, J. O.; Gerber, R. B. *J. Chem. Phys.* **1996**, *105*, 10682.
(48) Jung, J. O.; Gerber, R. B. *J. Chem. Phys.* **1996**, *105*, 10332.
(49) Maslen, P. E.; Handy, N. C.; Amos, R. D.; Jayatilaka, P. *J. Chem. Phys.* **1992**, *97*, 4233.
(50) Bludsky, O.; Spirko, V.; Kobayashi, R.; Jørgensen, P. *Chem. Phys. Lett.* **1994**, *228*, 568.
(51) Bludsky, O.; Bak, K. L.; Jørgensen, P.; Spirko, V. *J. Chem. Phys.* **1995**, *103*, 10110.
(52) Skokov, S.; Peterson, K. A.; Bowman, J. M. *J. Chem. Phys.* **1998**, *109*, 2662.
(53) Persson, B. J.; Taylor, P. R.; Martin, J. M. L. *J. Phys. Chem. A* **1998**, *102*, 2483.
(54) Chaban, G. M.; Gerber, R. B.; Jung, J. O. *J. Chem. Phys.* **1999**, *111*, 1823.
(55) Chaban, G. M.; Gerber, R. B. *J. Chem. Phys.* **2001**, *115*, 1340.
(56) Gauss, J.; Stanton, J. F. *J. Phys. Chem. A* **2000**, *104*, 2865.
(57) Gauss, J.; Cremer, D.; Stanton, J. F. *J. Phys. Chem. A* **2000**, *104*, 1319.
(58) anf Gauss, J.; Bak, K. L.; Jørgensen, P.; Olsen, J.; Helgaker, T.; Stanton, J. F. *J. Chem. Phys.* **2001**, *114*, 6548.
(59) Stanton, J. F.; Lopreore, C. L.; Gauss, J. *J. Chem. Phys.* **1998**, *108*, 7190.
(60) Bowman, J. M. *J. Chem. Phys.* **1978**, *68*, 608.
(61) Gerber, R. B.; Ratner, M. A. *Chem. Phys. Lett.* **1979**, *68*, 195.
(62) Bowman, J. M. *Acc. Chem. Res.* **1986**, *19*, 202.
(63) Gerber, R. B.; Ratner, M. A. *Adv. Chem. Phys.* **1998**, *70*, 97.
(64) Johnson, R. D., III; Hudgens, J. F. *J. Phys. Chem.* **1996**, *100*, 19874.
(65) ACES II. Stanton, J. F.; Gauss, J.; Watts, J. D.; Lauderdale, W. J.; Bartlett, R. J. 1993. The package also contains modified versions of the MOLECULE Gaussian integral program of J. Almlöf and P. R. Taylor, the ABACUS integral derivative program written by T. U. Helgaker, H. J. Aa. Jensen, P. Jørgensen and P. R. Taylor, and the PROPS property evaluation integral code of P. R. Taylor.
(66) Kong, J.; White, C. A.; Krylov, A. I.; Sherrill, C. D.; Adamson, R. D.; Furlani, T. R.; Lee, M. S.; Lee, A. M.; Gwaltney, S. R.; Adams, T. R.; Daschel, H.; Zhang, W.; Korambath, P. P.; Ochsenfeld, C.; Gilbert, A. T. B.; Kedziora, G. S.; Maurice, D. R.; Nair, N.; Shao, Y.; Besley, N. A.; Maslen, P.; Dombroski, J. P.; Baker, J.; Bird, E. F. C.; Van Voorhis, T.; Oumi, M.; Hirata, S.; Hsu, C.-P.; Baker, J.; Challacombe, M.; Schwegler, E.; Dombroski, J. P.; Ochsenfeld, C.; Ishikawa, N.; Florian, J.; Adamson, R. D.; Warshel, A.; Johnson, B. G.; Gill, P. M. W.; Head-Gordon, M.; Pople, J. A. *J. Comput. Chem.* **2000**, *21*, 1532.
(67) Krishnan, R.; Binkley, J. S.; Seeger, R.; Pople, J. A. *J. Chem. Phys.* **1980**, *72*, 650.
(68) McLean, A. D.; Chandler, G. S. *J. Chem. Phys.* **1980**, *72*, 5639.
(69) Frisch, M. J.; Pople, J. A.; Binkley, J. S. *J. Chem. Phys.* **1984**, *80*, 3265.
(70) Clark, T.; Chandrasekhar, J.; Schleyer, P. V. R. *J. Comput. Chem.* **1983**, *4*, 294.
(71) LEVEL 7.1: A Computer Program for Solving the Radial Schrodinger Equation for Bound and Quasibound Levels. Roy, R. J. Le University of Waterloo Chemical Physics Research Report CP-642R 2000. The source code and manual for this program may be obtained from the www site *http://theochem.uwaterloo.ca/*~leroy.
(72) Fessenden, R. W.; Schuler, R. H. *J. Chem. Phys.* **1965**, *43*, 2704.
(73) The complete orbital following model assumes that the s-character of the unpaired electron is directly proportional to the OPLA angle Θ, as suggested by the hybridization theory. That is, from the orthogonality considerations for the hybrid orbital, the s-caracter of the unpaired electron is estimated to be 2 $\tan^2 \Theta$. Since the hyperfine interactions are much stronger for s-electrons (contrary to the higher angular momentum, s-orbitals do not have a node on the nucleus), the angular dependence of the carbon hyperfine coupling constant a_C is assumed to have the following form: $a_C(\Theta) = a_C(0) + A2 \tan^2 \Theta$, where $A \sim 1190$ G is the contribution from an electron on a 2s carbon orbital. Thus, complete orbital following predicts a strong increase in the a_C at the nonplanar geometries. The incomplete orbital following means that the s-character of the hybrid orbital containing the unpaired electron cannot be derived from the hybridization theory and, therefore, makes the dependence $a_C(\Theta)$ less dramatic.
(74) Schrader, D. M.; Karplus, M. *J. Chem. Phys.* **1964**, *40*, 1593.
(75) NBO 4.0. Glendening, E. D.; Badenhoop, J. K.; Reed, A. E.; Carpenter, J. E.; Weinhold, F. Theoretical Chemistry Institute, University of Wisconsin, Madison, WI, 1996.
(76) The larger incompleteness of the orbital following in CH_2F (as compared to the orbital following in CH_3) can be readily rationalized: the electrostatic attraction of the positively charged hydrogens to the negatively charged fluorine results in the additional stabilization of the nonplanar structure. Thus, the relative role of the orbital hybridization is smaller in CH_2F than in CH_3.
(77) Botschwina, P.; Flesch, J.; Meyer, W. *Chem. Phys.* **1983**, *74*, 321.
(78) Mebel, A. M.; Lin, S.-H. *Chem. Phys.* **1997**, *215*, 329.
(79) Dixon, D. A.; Feller, D.; Peterson, K. A. *J. Phys. Chem. A* **1997**, *101*, 9405.
(80) Zahedi, M.; Harrison, J. A.; Nibler, J. W. *J. Chem. Phys.* **1994**, *100*, 4043.
(81) Triggs, N. E.; Zahedi, M.; Nibler, J. W. *J. Chem. Phys.* **1992**, *96*, 1822.
(82) Kelly, P. B.; Westre, S. G. *Chem. Phys. Lett.* **1988**, *151*, 253.
(83) Holt, P. L.; McCurdy, K. E.; Weisman, R. B.; Adams, J. S.; Engel, P. S. *J. Chem. Phys.* **1984**, *81*, 3349.
(84) Tam, S.; Macler, M.; Fajardo, M. E. *J. Chem. Phys.* **1997**, *106*, 8955.
(85) Momose, T.; Miki, M.; Uchida, M.; Shimizu, T.; Yoshizawa, I.; Shida, T. *J. Chem. Phys.* **1995**, *103*, 1400.
(86) Amano, T.; Bernath, P. F.; Yamada, C.; Endo, Y.; Hirota, E. *J. Chem. Phys.* **1982**, *77*, 5284.
(87) Tanarro, I.; Sanz, M. M.; Bermejo, D.; Domingo, C.; Santos, J. *J. Chem. Phys.* **1994**, *100*, 238.
(88) Davis, S.; Duxbury, D. T. Anderson G.; Nesbitt, D. J. *J. Chem. Phys.* **1997**, *107*, 5661.
(89) Snelson, A. *J. Phys. Chem.* **1970**, *74*, 537.
(90) Pacansky, J.; Bargon, J. *J. Am. Chem. Soc.* **1975**, *97*, 6896.
(91) Yamada, C.; Hirota, E. *J. Mol. Spectrosc.* **1986**, *116*, 101.
(92) Raymond, J. I.; Andrews, L. *J. Phys. Chem.* **1971**, *75*, 3235.